Time-Resolved EPR Study of the Photophysics and Photochemistry of 1-(3-(Methoxycarbonyl)propyl)-1-phenyl[6.6]C_{61}

Thomas W. Hamann,[†] Nagarajan Srivatsan,[‡] and Hans van Willigen*

Department of Chemistry, University of Massachusetts at Boston, Boston, Massachusetts 02125

Received: July 12, 2005; In Final Form: September 29, 2005

Time-resolved (TR) EPR was used to study the photophysics and photochemistry of 1-(3-(methoxycarbonyl)-propyl)-1-phenyl[6.6]C_{61} (M1). The CW TREPR spectra of M1 in the photoexcited triplet state, frozen in a rigid matrix and in liquid solution at room temperature, were compared with those of $^3C_{60}$. The introduction of the substituent on C_{60} has a striking effect on the spectra of the triplets, which is attributed to the lifting of the orbital degeneracy by the reduction in symmetry. Fourier transform (FT) EPR was used in an investigation of electron-transfer reactions in liquid solutions mediated by ^{3}M1. Of particular interest was the system of M1/chloranil (CA)/ perylene (Pe). Photoexcitation of M1 is found to lead to the formation of the chloranil anion radical and the perylene cation radical. From the chemically induced dynamic electron polarization (CIDEP) patterns in the FTEPR spectra and the dependence of the reaction kinetics on reactant concentrations, it was deduced that CA^- is formed by two competing pathways following photoexcitation of M1: (1) direct electron transfer from ^{3}M1 to CA followed by electron transfer from Pe to $M1^+$ and (2) energy transfer from ^{3}M1 to Pe followed by oxidative quenching of ^{3}Pe by CA. In both pathways, M1 acts as a light-energy harvester and mediator of electron-transfer reactions from Pe to CA without itself being consumed in the process, that is, as a photocatalyst. It is found that the functionalization of C_{60} makes its triplet state a worse electron donor and acceptor, but it has no significant effect on the triplet energy transfer reaction.

1. Introduction

It has been found that C_{60} strongly absorbs visible light and that photoexcitation leads to the formation of relatively long-lived triplets ($^3C_{60}$) with nearly 100% quantum efficiency.[1] $^3C_{60}$ can undergo reversible electron-transfer reactions with both donors and acceptors. In the presence of a good electron acceptor, such as tetracyanoethylene,[2,3] tetracyanoquinodimethane,[3] or chloranil,[4] $^3C_{60}$ is oxidatively quenched. Alternatively, in the presence of donors such as tri-*p*-tolylamine or hydroquinone,[5] $^3C_{60}$ is reduced. Because of these unique properties, C_{60} is a promising candidate for use in applications such as solar photochemistry, photodynamic therapy, and optoelectronic devices.[6−10]

Of particular interest in this work is the use of $^3C_{60}$ as a photocatalyst of electron-transfer reactions between species that do not absorb visible light. The present study is an extension of an earlier Fourier transform (FT) EPR and flash photolysis study of the system C_{60}/chloranil (CA)/perylene (Pe), which established that photoexcited $^3C_{60}$ initiates fast and efficient electron-transfer reactions to CA by three distinct pathways.[4] The use of C_{60} as a photocatalyst in a homogeneous solution is somewhat complicated because it remains in solution with the product(s) of interest, which makes isolating the product(s) difficult. In addition, recovering the C_{60} for further use would be a tedious process. To explore the application of C_{60} in photocatalysis of electron-transfer reactions in heterogeneous media, where product isolation and catalyst recovery problems may be alleviated, a handle with a terminal ester or carboxylic acid group was attached to C_{60} following a literature procedure.[11] The acid form of the stable C_{60} adduct allows for attachment to solid supports such as silica gel or TiO_2, providing a photocatalysis system that can be recovered readily after use.

To understand the effect of the substituent on the characteristics of the EPR spectrum of $^3C_{60}$, the adduct 1-(3-(methoxycarbonyl)propyl)-1-phenyl[6.6]C_{61} (M1, structural formula) was synthesized[11] and studied. The time-resolved (TR) EPR spectra of ^{3}M1 in frozen toluene/chloroform (1:1) and in toluene at room temperature were compared with spectra of $^3C_{60}$ under similar conditions. The distinct features of the TREPR spectra given by ^{3}M1 in liquid solution and randomly oriented in frozen solution allow for a straightforward detection of the adsorption of the C_{60} adduct from solution onto a solid support such as a TiO_2 film.

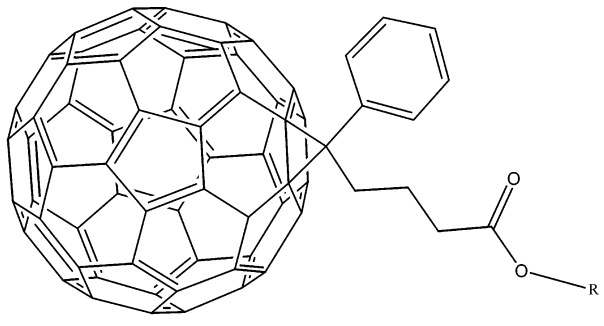

Structural formula: R = CH_3 in M1

FTEPR was used to investigate electron-transfer reactions in liquid solutions mediated by ^{3}M1. Of particular interest is the system M1/CA/Pe in benzonitrile. The study of the M1/CA/Pe

* To whom correspondence should be addressed. E-mail: hans.vanwilligen@umb.edu.

[†] Current address: California Institute of Technology, Division of Chemisty and Chemical Engineering, MC 127-72, 1200 E California Boulevard, Pasadena, California 91125.

[‡] Current address: Avery Research Center, Pasadena, California 91107.

10.1021/jp0538363 CCC: $30.25
Published on Web 11/23/2005

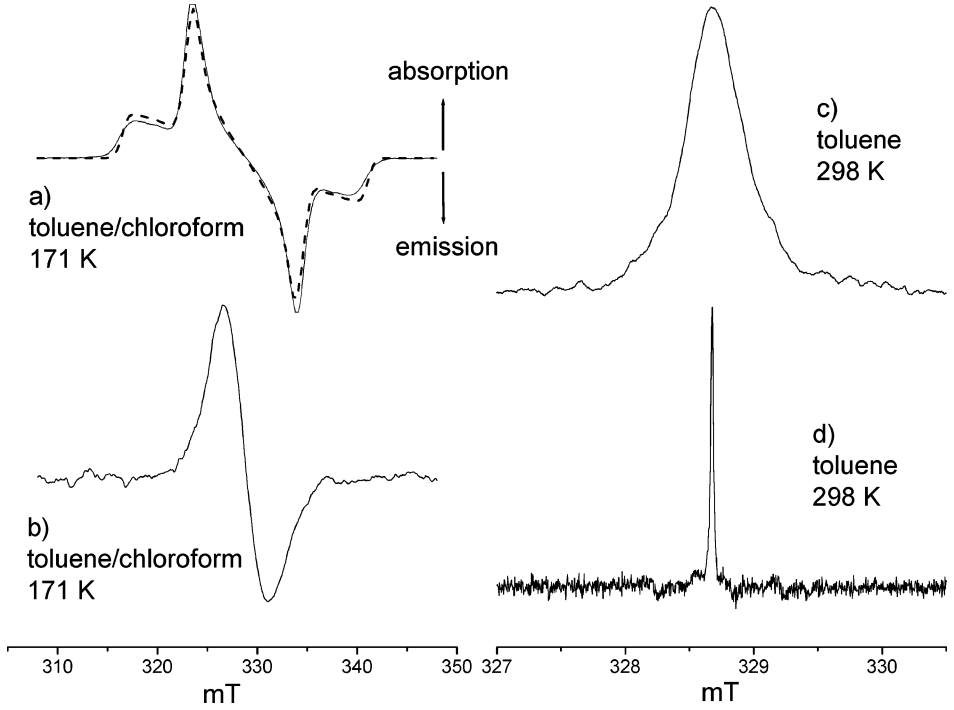

Figure 1. Rigid matrix CW TREPR spectra. (a) Photoexcited M1 in toluene/chloroform (1:1) at ~170 K, $\tau_d = 500$ ns. The dotted line represents the computer simulation of the spectrum with parameters given in Table 1. (b) Photoexcited C_{60} in toluene/chloroform (1:1) at ~170 K, $\tau_d = 200$ ns. CW TREPR spectra in fluid solution at room temperature. (c) ^{3}M1 in toluene at room temperature, $\tau_d = 800$ ns. (d) $^3C_{60}$ in toluene at room temperature, $\tau_d = 1$ μs.

system with FTEPR gives a great deal of insight into the mechanisms leading to electron transfer. This is because the spectra, in addition to providing data on chemical kinetics, show chemically induced dynamic electron polarization (CIDEP) effects[12] characteristic of the distinct reaction routes. It is found that ^{3}M1 acts as a visible-light photocatalyst by mediating electron-transfer reactions from Pe to CA without itself being consumed in the process.

2. Experimental Section

All solvents (highest grade available, Aldrich), perylene (gold label, Aldrich), and all chemicals required for the synthesis of M1 (Aldrich) were used as received. Chloranil (Aldrich) was purified by vacuum sublimation. M1 was prepared in accordance with a literature procedure[11] from C_{60} (99.9%, SES Research).

All samples were excited with the second harmonic (532 nm) of a Quanta Ray GCR 12 Nd:YAG laser (pulse width ~8 ns, pulse energy ~20 mJ, and 10 Hz repetition rate). CW TREPR measurements were carried out with a Varian E-9 X-band spectrometer equipped with a boxcar integrator for direct detection of EPR signals. A Varian variable-temperature accessory was utilized to set sample temperatures. Measurements were taken at temperatures ranging from 170 to 298 K. Samples were purged with argon to remove oxygen.

FTEPR measurements were carried out on a home-built spectrometer described previously.[13] The magnetic field was generated by a Varian 9 in. magnet. The microwave radiation was provided by a phase-locked source operating at 9.144 GHz amplified by a 1 kW TWT microwave amplifier. The MW pulse width is ~15 ns. The FID was detected with an IF quadrature mixer, and a CYCLOPS phase-cycling routine was employed to cancel the differences between the two channels.[14] All FTEPR measurements were carried out at room temperature. The recorded FIDs were the averages of signals generated by 2000 laser shots (500 per phase). Missing points in the FID due to the dead time of the instrument were calculated with an LP-SVD routine.[15] The signal phase was confirmed by comparison with the spectrum given by the tetracyanoethylene anion radical ($TCNE^-$) in 2-MTHF. Prior to the measurements, the samples were subjected to several freeze−pump−thaw cycles under high vacuum to remove oxygen, after which they were sealed off under vacuum.

The concentration of M1 was $\sim 1.5 \times 10^{-4}$ M for all measurements. The concentrations of CA and Pe were varied from 3.6×10^{-4} to 1.1×10^{-2} M and from 8.6×10^{-5} to 9.6×10^{-3} M, respectively. FTEPR spectra were recorded following the laser pulse with delay time settings (τ_d) ranging from 50 ns to 500 μs.

3. Results and Discussion

3.1. TREPR Spectra of ^{3}M1 and $^3C_{60}$. Figure 1a displays the rigid matrix (toluene/chloroform 1:1, ~171 K) CW TREPR spectrum given by ^{3}M1 for a 500 ns delay between laser excitation and signal detection. The spectrum exhibits the characteristic powder pattern caused by the dipolar interaction between the two unpaired electrons of the triplet.[16] The absorption/emission spin-polarization pattern in the spectrum reflects the spin selectivity of the intersystem crossing (isc) process. The dotted line in Figure 1a represents the computer simulation[17] of the spectrum given by ^{3}M1. The values of zero-field splitting parameters, D and E, the relative population rates of the zero-field spin states, p_x, p_y, and p_z, and the line width (full width at half-maximum (fwhm)) used in the simulation are given in Table 1 together with those derived from the $^3C_{60}$ spectra.[18]

A comparison with the spectrum given by $^3C_{60}$ under identical conditions (Figure 1b) illustrates the pronounced effect of the substituent. The orbital degeneracy of C_{60} in the first excited

TABLE 1: Parameters Used for the Simulation of CW TREPR Spectra of M1 Triplets in a Rigid Matrix at 170 K and Those Derived in an Earlier Analysis[18] of the Spectrum of $^3C_{60}$ Recorded at 4 K

parameters	M1 (170 K)	C_{60} (4 K)[18]
D (10^{-4} cm^{-1})	−115.	−114.
E (10^{-4} cm^{-1})	6.	5.
p_x	0.3	∼0.5
p_y	0.7	∼0.5
p_z	0	0
fwhm (mT)	0.6	

triplet state gives rise to a dynamic Jahn−Teller effect (pseudorotation) that at a temperature as low as 171 K already leads to a partial averaging of the zero-field splitting.[18] The substituent removes the orbital degeneracy so that in the case of ^{3}M1 a static rigid matrix spectrum is observed. However, introduction of the substituent does not noticeably affect the D and E values (cf. Table 1), which indicates that the electron spin distribution over the C_{60} moiety remains essentially unchanged.

The TREPR spectra of ^{3}M1 and $^3C_{60}$ in fluid solution at room temperature (cf. Figure 1c and 1d) also illustrate the dramatic effect that the loss of orbital degeneracy has on the resonance signal. In both systems, the zero-field splitting is almost completely averaged out. The narrow line width of the $^3C_{60}$ resonance is due to the fast averaging of the dipole−dipole interaction between the unpaired electrons by interconversion between Jahn−Teller states.[18,19] The CW TREPR spectrum of ^{3}M1 in toluene is significantly broader because of the absence of this pseudorotation mechanism.

The room-temperature CW TREPR spectrum given by ^{3}M1 (Figure 1c) was analyzed in some detail to extract parameters that could aid in the quantitative interpretation of the data given by the FTEPR study of electron-transfer reactions discussed in the next sections. The ^{3}M1 peak was fit to a Lorenzian with a value of 13 MHz for the fwhm. From this measured value, T_2 can be calculated according to $T_2 = (\pi \text{ fwhm})^{-1}$, which gives a value of $T_2 = 25$ ns. Because the dead time of the FTEPR spectrometer is ∼100 ns, the ^{3}M1 signal is not observable using FTEPR. In contrast, T_2 is approximately 500 ns for $^3C_{60}$, which, consequently, is observable using FTEPR.[20]

The line width of the EPR signal given by a rotating triplet is determined by the values of D and E and the rotational correlation time τ_c according to[21]

$$\frac{1}{T_2} = \frac{\Delta^2}{20}\left\{6\tau_c + \frac{10\tau_c}{1+\omega_0^2\tau_c^2} + \frac{4\tau_c}{1+4\omega_0^2\tau_c^2}\right\} \quad (1)$$

where $\Delta^2 = {}^2/_3(D^2 + 3E^2)/h^2$ is the zero-field splitting in rad/s and ω_0 is the Larmor frequency. Substituting the D and E values given in Table 1 and $T_2 = 25$ ns, a value of $\tau_c = 29$ ps was derived for ^{3}M1 in toluene. This is in close agreement with the value 22.8 ps predicted[22] for $^3C_{60}$ by the Stokes−Debye−Einstein equation

$$\tau_c = \frac{4\pi\eta a^3}{3k_BT} \quad (2)$$

where $\eta = 0.56$ cp, which is the viscosity of toluene at 25 °C,[23] $a = 0.35$ nm,[24] which is the molecular radius of C_{60}, k_B is the Boltzmann constant, and T is the temperature. The derived value $\tau_c = 29$ ps is also consistent with the NMR results that give $\tau_c = 16.9$ ps for $^3C_{60}$ in toluene at 303 K.[24] The slightly larger rotational correlation time of ^{3}M1 may reflect the effect of the addition of the substituent on the effective molecular radius and therefore τ_c. Because all of the electron-transfer reaction measurements were performed on solutions in the more polar solvent benzonitrile and the rotational correlation time is proportional to the viscosity of the solvent, τ_c for ^{3}M1 in benzonitrile can be estimated by multiplying τ_c in toluene by the ratio of the viscosities of benzonitrile ($\eta = 1.267$ cp at 25 °C[25]) and toluene. This gives an estimated value of $\tau_c \approx 65$ ps for ^{3}M1 in benzonitrile. In contrast, the pseudorotation effect reduces τ_c to ∼0.8 ps in the case of $^3C_{60}$ in toluene at 300 K.[22]

The spin−lattice relaxation time of ^{3}M1, T_1^T, can be calculated from the zero-field splitting parameters and the rotational correlation time according to[21]

$$\frac{1}{T_1} = \frac{\Delta^2}{10}\left\{\frac{2\tau_c}{1+\omega_0^2\tau_c^2} + \frac{8\tau_c}{1+4\omega_0^2\tau_c^2}\right\} \quad (3)$$

Using the estimated value of τ_c in benzonitrile (65 ps) and the D and E values from Table 1, a value of 214 ns for T_1^T in benzonitrile was derived.

The initial spin polarization P of the M1 triplets produced by the spin-selective intersystem crossing is given by[26]

$$P = \frac{2}{15}\left(\frac{2\pi k_BT}{h\omega}\right)(D^*\omega\tau_c^{\,2})K[4(1+(2\omega\tau_c)^2)^{-1} + (1+(\omega\tau_c)^2)^{-1}] \quad (4)$$

In this equation, $D^* = (D^2 + 3E^2)/2$, $K = [(p_x + p_y)/2 - p_z]$, and the term $2\pi k_BT/h\omega$ is introduced to give the polarization with respect to the thermal equilibrium value (P_B).[21] Substituting the D, E, p_x, p_y, and p_z values given in Table 1, the calculated rotational correlation time (65 ps), and a frequency of 9.218 GHz, a value of $P = 3.3$ was found. In contrast, $^3C_{60}$ is generated with a polarization of approximately 0.1−0.2 with respect to Boltzmann.[22] The drastic difference in P is consistent with the reduction in the value of τ_c on going from ^{3}M1 to $^3C_{60}$.

The data derived from the CW TREPR spectra of $^3C_{60}$ and ^{3}M1 are useful in the consideration of the FTEPR study of the M1/CA and M1/CA/Pe systems. First, the pronounced differences in line widths of the liquid solution triplet spectra (cf. Figure 1) indicate that the kinetics of triplet quenching by electron or energy transfer can be monitored via the narrow-line $^3C_{60}$ FTEPR signal, whereas the ^{3}M1 signal cannot be observed. Furthermore, according to the interpretation of the TREPR data, M1 triplets are born with $P \approx 3.3P_B$. This spin polarization will be carried over to electron-transfer products if the rate of electron transfer competes with the triplet spin−lattice relaxation rate, $1/T_1^T \approx 4.7 \times 10^6$ s^{-1}, giving rise to triplet mechanism (TM) CIDEP.[12,27]

3.2. FTEPR of M1 with Chloranil and Perylene.

A. M1/Chloranil. Photoexcitation of solutions of M1 in the presence of CA in benzonitrile results in the reversible formation of a free radical, giving rise to FTEPR spectra with a single resonance peak. The signal is assigned to CA^- on the basis of the g value (2.0057).[4] The CA anion radical is formed by electron transfer from ^{3}M1. The CA^- resonance peak is in absorption at all delay times. No resonance peak was observed for ^{3}M1 or $M1^+$, which is attributed to the short T_2 of these species. A representative FTEPR spectrum and the time profile of the intensity of the CA^- resonance are shown in Figure 2.

During the course of a series of measurements with different delay time settings, an additional peak is observed growing in gradually. On the basis of the g factor (2.0012) and line width, this resonance was assigned to $^3C_{60}$.[19,20] Because the peak grows

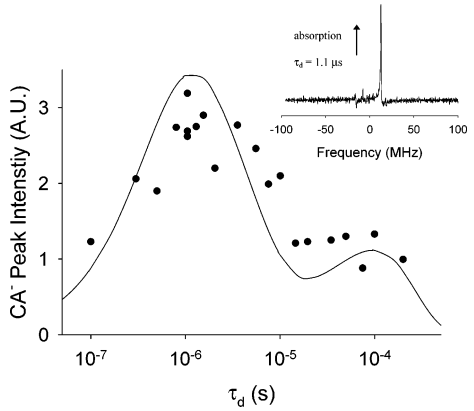

Figure 2. Time profile of the FTEPR CA^- signal intensity for the M1/CA (4.3×10^{-3} M) system in benzonitrile following a 532 nm laser pulse. The solid line is a simulation (see text) using the parameters in Table 2. The inset shows the FTEPR spectrum for a 1.1 μs delay between laser excitation and microwave pulse.

in slowly during a series of measurements, each requiring 2000 laser shots, the decomposition apparently represents a side reaction in which a small fraction of $M1^+$ decomposes to C_{60} before the back electron-transfer reaction regenerates M1. This interpretation is supported by the finding that the decomposition reaction can be inhibited by adding pyrene (Py) to the solution. Pyrene was chosen because it is a good electron donor and can intercept the M1 cation radical before decomposition can occur via the reaction

$$M1^+ + Py \rightarrow M1 + Py^+$$

The triplet energy of Py ($E_T = 2.1$ eV)[28] is significantly higher than that of ^{3}M1 ($E_T \approx 1.5$ eV[29,30]); therefore, it should not interfere with the oxidative quenching of ^{3}M1 by CA. This expectation is supported by the observation that the presence of Py does not appear to affect the time profile of the CA^- resonance with the exception of a reduction in data scatter.

Whereas the M1/CA system gives rise to an absorption peak, the CA^- signal produced by the C_{60}/CA system is in emission at early times.[4] As noted in section 3.1, photoexcitation of C_{60} produces triplets with spin polarization far below the thermal equilibrium value. For this reason, the emissive signal given by CA^- produced in the electron-transfer reaction

$$^3C_{60} + CA \rightarrow [C_{60}^+ \cdots CA^-] \rightarrow C_{60}^+ + CA^-$$

was attributed[4] to the polarization generated by the spin state evolution of the transient radical pair $[C_{60}^+ \cdots CA^-]$ (radical pair mechanism (RPM) CIDEP[12]). In the system M1/CA, by contrast, the CA^- signal intensity is determined by the spin polarization transferred from ^{3}M1. Because the value of the triplet T_1 is predicted to be relatively high (214 ns, cf. section 3.1), the triplet spin polarization persists long enough for TM CIDEP[12,27] to play a dominant role.

As the C_{60} concentration increases and M1 decreases because of the decomposition of $M1^+$, the parallel electron-transfer reaction involving $^3C_{60}$ attenuates the absorptive CA^- signal. It is a source of the significant scattering of data in the time profile of CA^- signal intensity displayed in Figure 2. For this reason, no attempt was made to analyze the time dependence quantitatively. Superimposed on the data, however, is a simulated time profile of the CA^- signal. The simulation is based on (a) the values of the initial triplet spin polarization $P = 3.3$ and triplet spin−lattice relaxation rate $k_{T1}^T \approx 4.7 \times 10^6$ s^{-1} derived from the CW TREPR data on ^{3}M1 (cf. section 3.1), (b) the published[4] relaxation rate of the CA^- spin system $k_{T1}^D = 1.9 \times 10^5$ s^{-1}, and (c) the values of the electron-transfer rate constant $k_{et} = 1.5 \times 10^6$ M^{-1} s^{-1} and the pseudo-first-order radical decay rate $k_d = 1 \times 10^4$ s^{-1} derived from the analysis described in section 3.2 C.

In flash photolysis studies of C_{60}/CA in benzonitrile, it was found that even though $^3C_{60}$ is quenched by CA no transient absorption peaks due to the redox products C_{60}^+ and CA^- were evident.[4,31] On the basis of this finding and the fact that the estimated $\Delta G°$ for the electron-transfer reaction is positive ($\Delta G° \approx 0.04$ eV[4]), Fukuzumi et al. concluded that no electron-transfer products were generated in the quenching process.[31] However, the data given by the FTEPR measurements provide unequivocal evidence that this conclusion is not correct. FTEPR shows the formation of CA^-, identified by its characteristic resonance peak, at a rate that corresponds within experimental uncertainty to the rate of quenching of $^3C_{60}$ as measured by flash photolysis.[4,31] Furthermore, the CIDEP features in the FTEPR spectra clearly show that CA^- is formed via a $^3C_{60}$...CA encounter. The results obtained in the FTEPR measurements on M1/CA in benzonitrile reaffirm this conclusion. In this system, the time evolution of the CA^- resonance peak reflects the unique spin polarization of the precursor ^{3}M1. The fact that flash photolysis failed to detect C_{60}^+ and CA^- can be attributed to the fact that contributions of these redox products to the transient absorption spectrum may be masked by spectral features due to other species. In the case of FTEPR, only paramagnetic molecules are detected, and in the systems considered here, there is no overlap of resonance peaks so that CA^- concentrations down to 10^{-5} M or lower can be readily detected. Even if only a small fraction of the triplet quenching events lead to the cage escape of electron-transfer products, the high sensitivity of the magnetic resonance technique makes it possible to detect the anion radicals generated.

B. M1/Perylene and Perylene/Chloranil. The measurements of M1/Pe samples in benzonitrile ([Pe] $= 1.1 \times 10^{-3}$ M) failed to give an FTEPR signal irrespective of the delay time setting. Because the Pe cation radical is observable with FTEPR,[4] this establishes that there is no electron transfer from Pe to ^{3}M1. In contrast, it was found previously that Pe is oxidized by $^3C_{60}$.[4] This difference is in accord with published thermodynamic data. For the reductive quenching reaction involving $^3C_{60}$ in benzonitrile, $\Delta G°$ has been estimated to be -0.13 eV.[4] This value is based on the 1.52 V[4] difference in the oxidation potential of Pe relative to the reduction potential of C_{60}, a C_{60} triplet energy of 1.57 eV,[32] and the assumption that the acceptor−donor distance is ~7 Å.[33] The reduction potential of M1 is reported[11] to be 113 mV more negative than that of C_{60} (both measured in *o*-dichlorobenzene), and the triplet energy of monoadduct derivatives of C_{60} is 1.50 eV.[29,30] Hence, $\Delta G°$ for the reductive quenching of ^{3}M1 by Pe is estimated to be ~0.05 eV. According to these data, the introduction of the substituent turns this electron-transfer reaction into a slightly uphill process.

Measurements of the Pe/CA system also failed to give FTEPR signals.

C. M1/Chloranil/Perylene. As illustrated in Figure 3, the addition of Pe to the M1/CA system makes a dramatic difference in the FTEPR spectra. The spectra show a single resonance peak due to CA^- and a weak multiline signal due to the Pe^+ radical. The time profile of the CA^- peak was followed for delay times varying from fifty nanoseconds to several hundreds of micro-

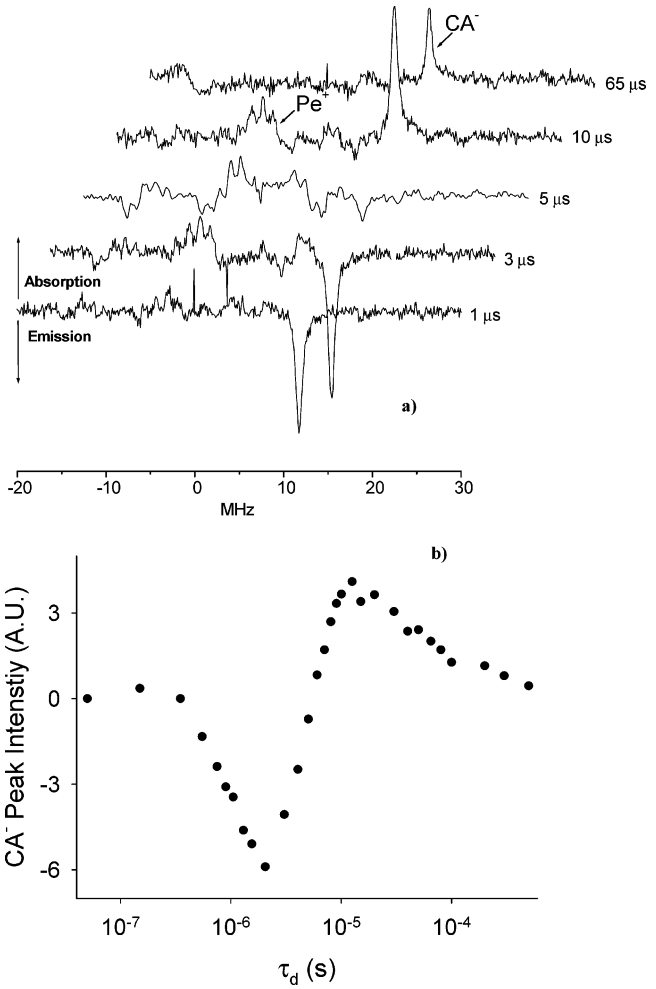

Figure 3. (a) FTEPR spectra given by M1/CA (4.3 × 10−3 M)/Pe (1.0 × 10−3 M) in benzonitrile, showing resonance peaks from CA^- and Pe^+, at delay times ranging from 1−65 μs following a 532 nm laser pulse. (b) Time profile of CA^- resonance peak intensity for this system.

seconds. The following two reaction routes can be invoked to account for the formation of these radicals:[4]

$$\text{I. } {}^3\text{M1} + \text{CA} \rightarrow [\text{M1}^+\cdots\text{CA}^-] \rightarrow \text{M1}^+ + \text{CA}^-$$

$$\text{M1}^+ + \text{Pe} \rightarrow \text{M1} + \text{Pe}^+$$

$$\text{II. } {}^3\text{M1} + \text{Pe} \rightarrow \text{M1} + {}^3\text{Pe}$$

$${}^3\text{Pe} + \text{CA} \rightarrow [\text{Pe}^+\cdots\text{CA}^-] \rightarrow \text{Pe}^+ + \text{CA}^-$$

Both reaction channels have the common back electron-transfer reaction

$$\text{Pe}^+ + \text{CA}^- \xrightarrow{k_d} \text{Pe} + \text{CA}$$

which makes the photoinduced processes fully reversible.

As shown in Figure 3, for the system M1/CA (4.3 × 10^{-3} M)/Pe (1.0 × 10^{-3} M) in benzonitrile, the CA^- resonance peak is initially in emission and turns into absorption after approximately 5 μs. Evidently, at these concentrations of CA and Pe, direct electron transfer from ^{3}M1 (route I) is not the primary route of CA^- formation because this has been shown to give rise to a CA^- resonance in absorption at all times. The fact that the CA^- resonance is in emission at early times points to formation via route II. The emissive signal from CA^- can be accounted for by the spin state evolution during the lifetime of

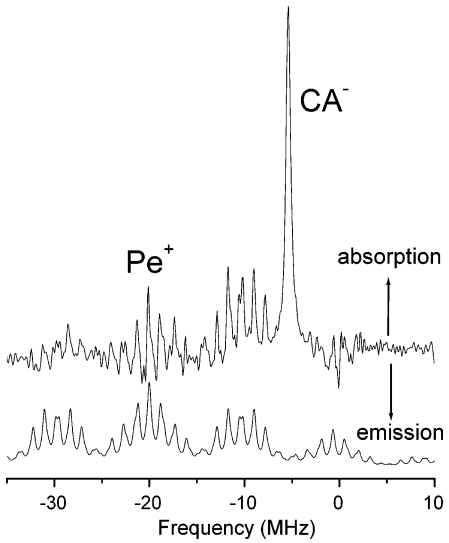

Figure 4. FTEPR spectrum given by M1/CA (1.1 × 10^{-2} M)/Pe (3.4 × 10^{-4} M) in benzonitrile, 10 μs after a 532 nm laser pulse. The spectrum is the result of 4000 laser shots (1000 per phase). The spectrum of Pe^+ shows the characteristic absorption/emission pattern generated by the RPM. At the bottom is the simulated spectrum of Pe^+ based on published hyperfine coupling data.

the radical pair [$Pe^+\cdots CA^-$] formed by the electron-transfer quenching of ^{3}Pe. The finding that the resonance peaks due to Pe^+ are in absorption on the low-frequency side of the CA^- peak and in emission on the other side (cf. Figure 4) is a characteristic feature of RPM CIDEP[12] and establishes unequivocally that CA^- and Pe^+ are formed in a common reaction step. A value of $T_1^T = 3$ ns was calculated for ^{3}Pe in benzonitrile using eq 3, substituting the values $\Delta = 1.7 \times 10^{10}$ rad/s[28] and $\tau_c = 72$ ps (calculated with eq 2 using $a = 0.38$ nm). Given this short T_1^T, radical formation via electron-transfer quenching of ^{3}Pe should not result in products with TM spin polarization.

In terms of the time dependence of the CA^- signal intensity at early times, the direct electron-transfer process (route I) should be identical to that for the M1/CA system described in section 3.2 A. However, with Pe present at a low enough concentration so that the contribution from route II is negligible, no signal from $^3C_{60}$ developed over the course of a series of measurements. Apparently, the presence of Pe leads to the rapid reduction of $M1^+$, which prevents the decomposition of $M1^+$ into C_{60} found in the M1/CA system. The initial absorption signal observed when [CA] > [Pe] is ascribed to TM CIDEP,[12,27] where the initial spin polarization of ^{3}M1 is carried over to CA^- at early times.

The time evolution of the intensity of the FTEPR signal due to CA^-, inclusive of both pathways of CA^- generation and their respective CIDEP mechanisms, is described by the general kinetic steps sketched in Scheme 1. In this scheme, it is assumed that the three triplet sublevels of ^{3}M1 react at the same rate, that RPM CIDEP plays a negligible role in route I, and that spin alignment is conserved in this CA^- formation step in accord with the TM CIDEP.[12,27] The fact that electron transfer from triplets at thermal equilibrium produces doublet radicals that are born with a spin polarization that is $^4/_3$ of the Boltzmann value[13] is also implicitly accounted for in the scheme. As noted earlier, the T_1 of ^{3}Pe is short so that electron-transfer quenching by CA cannot compete with the relaxation of the triplet spin system to thermal equilibrium. Consequently, the CIDEP signal contribution due to CA^- formation via route II is attributed entirely to the spin state evolution of the [$CA^-\cdots Pe^+$] radical pair. In the reaction scheme, this RPM CIDEP contribution is

SCHEME 1: General Kinetic Scheme, Including Spin Selective Steps, of the Two Pathways of CA^- Formation in the M1/CA/Pe System[a]

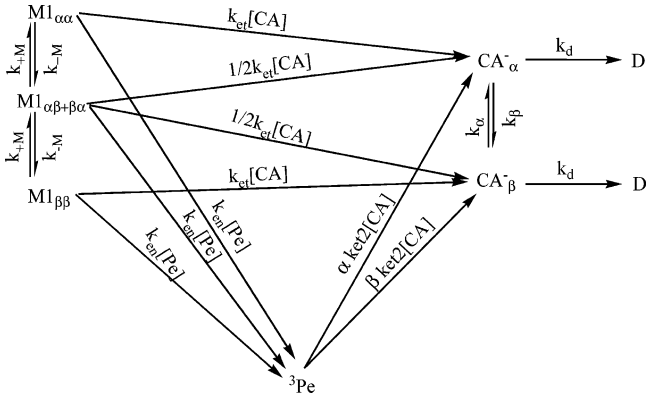

[a] (1) Direct electron transfer from ^{3}M1 to CA and (2) energy transfer from ^{3}M1 to Pe followed by electron transfer from ^{3}Pe to CA.

accounted for in terms of distinct population rate constants, αk_{et2} and βk_{et2} with $\alpha + \beta = 1$, of the α and β spin states of the anion radical.

Because of the complicated nature of this scheme, a general analytic solution was not possible. Instead, the resulting system of differential equations was represented in matrix format and solved numerically. Under the conditions of the measurements, $[^3M1] \ll [CA], [Pe]$ so that the reaction steps involving CA and Pe can be treated as pseudo-first-order processes (indicated by the rate constants with primes in the matrix). In addition, the signal decay due to the second-order back electron-transfer reaction was approximated as a first-order process because this greatly simplifies the analysis and is not expected to affect the time evolution of the CA^- signal for the first $10-20$ μs, which is of primary interest.

The extraction of reliable values of the rate constants of interest here, k_{et} and k_{en}, from the time profiles of the CA^- signal intensity by this method is greatly facilitated by the knowledge of the values of most of the parameters in the rate scheme. The initial relative concentrations of the triplet sublevels of ^{3}M1 are derived from the calculated relative isc population rates (cf. Table 1). The rate constants k_α and k_β are determined from the relationships $k_\alpha + k_\beta = k_{T1}^D = 1.9 \times 10^5$ s^{-1} [4] and $k_\alpha/k_\beta = \exp(-\Delta E/k_BT) = 0.9985$. The rate constants k_{+M} and k_{-M} are analogously determined from $k_{+M} + k_{-M} = k_{T1}^T = 4.7 \times 10^6$ s^{-1} (cf. section 3.1) and $k_{+M}/k_{-M} = \exp(-\Delta E/k_BT) = 0.996$. The published[4] electron-transfer rate constant from ^{3}Pe to CA, $k_{et2} = 5.6 \times 10^9$ M^{-1} s^{-1}, was also used as a fixed parameter in the least-squares analysis. A value of $k_d = 1 \times 10^4$ s^{-1} was obtained by fitting the data for $\tau_d > 20$ μs given by systems with [Pe] > [CA] to a first-order decay with the assumption that the CA^- spin system is at thermal equilibrium and that quenching of ^{3}M1 is essentially complete. The error associated with this parameter results in negligible differences in the fit results reported below.

The parameters k_{et}, k_{en}, and $(\beta - \alpha)$ were treated as floating parameters in a nonlinear least-squares fit of each data set to eq 5, keeping all other parameters fixed at the values given above. The resulting values and error margins of the rate constants are given in Table 2. The value reported for k_{et} represents the average of values from fits of five sets of data with [CA] and [Pe] chosen so that the CA^- signal is in absorption at early times, which indicates a dominating contribution from route I. Representative examples of fit results are given in Figure 5a−c.

A value of $k_{et} = (1.5 \pm 0.6) \times 10^6$ M^{-1} s^{-1} was found, which is an order of magnitude smaller than the rate constant for electron transfer found from $^3C_{60}$ to CA.[4] The reduction in the rate constant by a factor of 10 suggests that the introduction of the substituent reduces the driving force of the oxidative electron-transfer reaction of the triplet state. The oxidation potential of M1 has not been measured, but that of a compound with a similar fullerene structure, Ph_2C_{61}, is reported[35] to be 190 mV lower than that of C_{60}. If a similar reduction in oxidation potential applies for M1, assuming a triplet energy of 1.50 eV[29,30], then $\Delta G° \approx -0.08$ eV for the reaction

$$^3M1 + CA \rightarrow M1^+ + CA^-$$

which suggests that the rate constant should exceed that of the reaction involving $^3C_{60}$, where $\Delta G° \approx 0.04$ eV. The discrepancy between the experimental result and the prediction based on these $\Delta G°$ values is not understood at this time. Interestingly, however, the value of $k_{et} = (1.5 \pm 0.6) \times 10^6$ M^{-1} s^{-1} determined here is similar to values of $k_{et} \approx (2-6) \times 10^6$ M^{-1} s^{-1} found for electron transfer from various triplet-state fullerene derivatives to CA in the presence of scandium trifluoromethanesulfonate.[31]

The value reported for k_{en} represents the average of values from the fitting of seven sets of data with a CA^- signal in emission (e.g., Figure 5c−e) where route II plays a dominant role. A value of $k_{en} = (8 \pm 3) \times 10^8$ M^{-1} s^{-1} was found, which

$$\begin{bmatrix} M1_{\alpha\alpha} \\ M1_{\alpha\beta+\beta\alpha} \\ M1_{\beta\beta} \\ {}^3Pe \\ CA_\alpha^- \\ CA_\beta^- \\ D' \end{bmatrix} =$$

$$\begin{bmatrix} -(k_{et}' + k_{en}' + k_{-M}) & k_{+M} & 0 & 0 & 0 & 0 & 0 \\ k_{-M} & -(k_{et}' + k_{en}' + k_{-M} + k_{+M}) & k_{+M} & 0 & 0 & 0 & 0 \\ 0 & k_{-M} & -(k_{et}' + k_{en}' + k_{+M}) & 0 & 0 & 0 & 0 \\ k_{en}' & k_{en}' & k_{en}' & k_{et2}' & 0 & 0 & 0 \\ k_{et}' & {}^1/_2 k_{et}' & 0 & \alpha k_{et2}' & -(k_d + k_\beta) & k_\alpha & 0 \\ 0 & {}^1/_2 k_{et}' & k_{et}' & \beta k_{et2}' & k_\beta & -(k_d + k_\alpha) & 0 \\ 0 & 0 & 0 & 0 & k_d & k_d & 0 \end{bmatrix} \begin{bmatrix} M1_{\alpha\alpha} \\ M1_{\alpha\beta+\beta\alpha} \\ M1_{\beta\beta} \\ {}^3Pe \\ CA_\alpha^- \\ CA_\beta^- \\ D \end{bmatrix} \quad (5)$$

TABLE 2: Rate Constants Determined from Nonlinear Least-Squares Fits of CA^- Intensity vs Delay Time Data Based on the Kinetic Diagram Given in Scheme 1[a]

process	rate constant for M1	rate constant for C_{60}[c]
$^3M1$ spin−lattice relaxation, $k_{T_1}^T$	4.6×10^6 s^{-1} [b]	2.7×10^6 s^{-1}
$^3M1 + CA \xrightarrow{k_{et}} M1^+ + CA^-$	$(1.5 \pm 0.6) \times 10^6$ M^{-1} s^{-1}	1.8×10^7 M^{-1} s^{-1}
$^3M1 + Pe \xrightarrow{k_{en}} M1^+ + {}^3Pe$	$(8 \pm 3) \times 10^8$ M^{-1} s^{-1}	1.2×10^9 M^{-1} s^{-1}
$^3Pe + CA \xrightarrow{k_{et2}} Pe^+ + CA^-$	5.6×10^9 M^{-1} s^{-1} [c]	5.6×10^9 M^{-1} s^{-1}
CA^- spin−lattice relaxation, $k_{T_1}^D$	1.9×10^5 s^{-1} [c]	1.9×10^5 s^{-1}

[a] The third column gives the corresponding rate constants found with C_{60} as sensitizer.[4] [b] Calculated value (eq 3). [c] Values taken from ref 4.

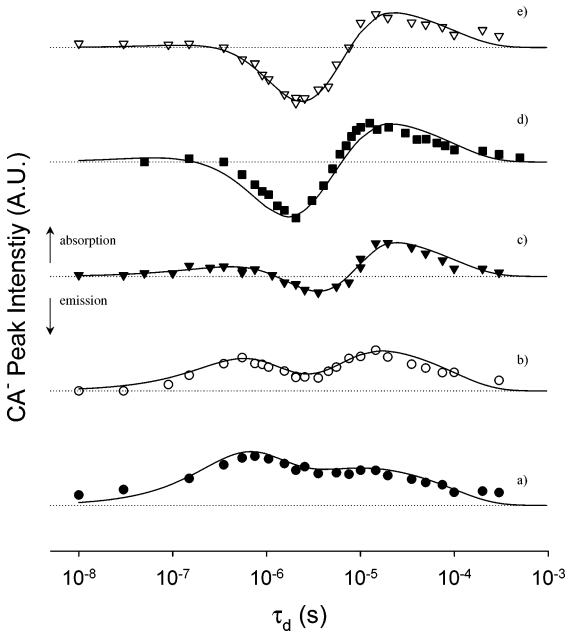

Figure 5. Time profiles of FTEPR CA^- signal intensities for the M1/CA/Pe system in benzonitrile following a 532 nm laser pulse for the following CA and Pe concentrations: (a) [CA] = 1.1×10^{-2} M, [Pe] = 3.4×10^{-4} M, ●; (b) [CA] = 1.1×10^{-2} M, [Pe] = 6.0×10^{-4} M, ○; (c) [CA] = 4.3×10^{-3} M, [Pe] = 3.4×10^{-4} M, ▲; (d) [CA] = 4.3×10^{-3} M, [Pe] = 1.0×10^{-3} M, ■; and (e) [CA] = 5.7×10^{-4} M, [Pe] = 1.0×10^{-3} M, △. The solid lines represent least-squares fits based on Scheme 1 using the parameters given in Table 2 and the text. The dotted lines indicate the zero-intensity level for each of the time profiles.

is essentially the same as the value reported for the rate constant of triplet energy transfer from $^3C_{60}$ to Pe.[4] This is in accord with previous conclusions that the derivatization of C_{60} has little effect on the triplet energy.[29,30,34,35] The quantity $(\beta - \alpha)$ was determined to be -1.7×10^{-3}, which indicates an emissive CA^- signal generated from route II with approximately twice the Boltzmann polarization.

Figure 5 illustrates that the nonlinear least-squares fit based on Scheme 1 with k_{et}, k_{en}, and $(\beta - \alpha)$ as adjustable parameters fits the data sets remarkably well for a wide range of CA (3.6×10^{-4} to 1.1×10^{-2} M) and Pe (8.6×10^{-5} to 9.6×10^{-3} M) concentrations. Furthermore, simulations of route I, using the parameters extracted from the nonlinear least-squares fit results, are consistent with the data of the M1/CA system as shown in Figure 2.

4. Conclusions

It was found that the addition of a substituent to C_{60} had a significant effect on its photophysical properties. The reduction of symmetry leads to strikingly different triplet TREPR spectra for M1 in a rigid matrix and in liquid solution. $^3M1$, like $^3C_{60}$, is able to mediate electron-transfer reactions following photoexcitation, but with significant differences.

First, no electron transfer was observed from Pe to $^3M1$, whereas it was found previously that $^3C_{60}$ is readily reduced by Pe as evident from the characteristic transient optical absorption and FTEPR signals from Pe^+.[4] However, the rate of triplet energy transfer to Pe is not affected much by the introduction of the substituent. These findings are in agreement with data in the literature that show that the effect of the substituent on the reduction potential of the C_{60} moiety (−0.113 V) far exceeds the effect on the triplet energy (−0.07 eV).[11,29,30] Second, the rate constant for electron transfer from $^3M1$ to CA, k_{et}, is found to be an order of magnitude smaller than that from $^3C_{60}$ to CA (cf. Table 2). This result conflicts with the expectation that oxidation of the fullerene becomes easier upon derivatization.[31]

As noted in the Introduction, the objective of introducing the handle with a terminal acid or ester group is to be able to anchor the photosensitizer on a solid support. The present study focuses exclusively on the properties of M1 in homogeneous solutions. However, CW TREPR measurements established[36] that the acid derivative is readily bound to TiO_2 and silica particles. A solution of the acid form of M1 in toluene was pumped through a flat quartz EPR cell with the insides of the windows coated with a TiO_2 film. Alternatively, silica gel was introduced into a solution of M1 in toluene. In both cases, it was observed that the triplet spectrum changed from that found in a fluid solution (cf. Figure 1c) to that found in a solid solution spectrum (Figure 1a). In contrast, in the ester form no adsorption from solution was found. This allows for the continuous monitoring of the physical state of M1 by means of the characteristics of the CW TREPR spectrum of its triplet state. This experimental arrangement should allow the use of FTEPR to monitor electron-transfer reactions in liquid solution photocatalyzed by M1 bound to a solid support.

Acknowledgment. We thank Professor John C. Warner of the University of Massachusetts at Lowell for help with the synthesis of the substituted C_{60} compounds. Financial support was provided by the Division of Chemical Sciences, Office of Basic Energy Sciences, of the U.S. Department of Energy (DE-FG02-84ER-13242).

References and Notes

(1) Arborgast, J. W.; Darmanyan, A. P.; Foote, C. S.; Rubin, Y.; Diederich, F. N.; Alvarez, M. M.; Anz, S. J.; Whetten, R. L. *J. Phys. Chem.* **1991**, *95*, 11−12.

(2) Michaeli, S.; Meiklyar, V.; Schulz, M.; Möbius, K.; Levanon, H. *J. Phys. Chem.* **1994**, *98*, 7444−7447.

(3) Nadtochenko, V. A.; Denisov, N. N.; Rubtsov, I. V.; Lobach, A. S.; Moravskii, A. P. *Chem. Phys. Lett.* **1993**, *208*, 431−435.

(4) Steren, C. A.; van Willigen, H.; Biczók, L.; Gupta, N.; Linschitz, H. *J. Phys. Chem.* **1996**, *100*, 8920−8926.

(5) Biczók, L.; Linschitz, H.; Walter, R. I. *Chem. Phys. Lett.* **1992**, *195*, 339−346.

(6) Hagfeldt, A.; Grätzel, M. *Acc. Chem. Res.* **2000**, *33*, 269−277.

(7) Grätzel, M. *J. Photochem. Photobiol., A* **2004**, *164*, 3−14.
(8) Somani, P. R.; Radhakrishnan, S. *Mater. Chem. Phys.* **2003**, *77*, 117−133.
(9) Nyman, E. S.; Hynninen, P. H. *J. Photochem. Photobiol., B* **2004**, *73*, 1−28.
(10) Jensen, A. W.; Wilson, S. R.; Schuster, D. I. *Bioorg. Med. Chem.* **1996**, *4*, 767.
(11) Hummelen, J. C.; Knight, B. W.; Lepeq, F.; Wudl, F.; Yao, J.; Wilkins, C. L. *J. Org. Chem.* **1995**, *60*, 532−538.
(12) McLauchlan, K. A. In *Modern Pulsed and Continuous Wave Electron Spin Resonance*; Kevan, L., Bowman, M. K., Eds.; Wiley: New York, 1990.
(13) Levstein, P. R.; van Willigen, H. *J. Chem. Phys.* **1991**, *95*, 900−908.
(14) Derome, A. E. *Modern NMR Techniques for Chemistry Research*; Pergamon Press: New York, 1987.
(15) Barkhuijsen, H.; de Beer, R.; Bovée, W.; van Ormondt, D. *J. Magn. Reson.* **1985**, *61*, 465−481.
(16) Weil, J. A.; Bolton, J. R.; Wertz, J. E. *Electron Paramagnetic Resonance*; Wiley: New York, 1994; p 167.
(17) Kottis, P.; Levebvre, R. *J. Chem. Phys.* **1963**, *39*, 393.
(18) Bennati, M.; Grupp, A.; Mehring, M. *J. Chem. Phys.* **1995**, *102*, 9457−9464.
(19) Closs, G. L.; Gautam, P.; Zhang, D.; Krusic, P. J.; Hill, S. A.; Wasserman, E. *J. Phys. Chem.* **1992**, *96*, 5228−5231.
(20) Steren, C. A.; Levstein, P. R.; van Willigen, H.; Linschitz, H.; Biczók, L. *Chem. Phys. Lett.* **1993**, *204*, 23−28.
(21) Carrington, A.; McLachlan, A. D. *Introduction to Magnetic Resonance*; Harper & Row: New York, 1967.
(22) Steren, C. A.; van Willigen, H.; Dinse, K. P. *J. Phys. Chem.* **1994**, *98*, 7464−7469.
(23) Landolt Börnstein, Vol. II/5a, p 160.
(24) Jones, V. K.; Rodriguez, A. A. *Chem. Phys. Lett.* **1992**, *198*, 373−378.
(25) *CRC Handbook of Chemistry and Physics*, 81st ed.; Lide, D. R., Ed.; CRC Press: Boca Raton, FL, 2001.
(26) Atkins, P. W.; Evans, G. T. *Mol. Phys.* **1974**, *27*, 1633−1644.
(27) Wan, J. K. S.; Wong, S. K.; Hutchinson, D. A. *Acc. Chem. Res.* **1974**, *7*, 58−64.
(28) *Handbook of Photochemistry*; Murov, S. L., Carmichael, I., Hug, G. L., Eds.; Marcel Dekker: New York, 1993.
(29) Luo, C.; Fujitsuka, M.; Watanabe, A.; Ito, O.; Gan, L.; Huang, Y.; Huang, C. H. *J. Chem. Soc., Faraday Trans.* **1998**, *94*, 527.
(30) Guldi, D. M.; Asmus, K. D. *J. Phys. Chem. A* **1997**, *101*, 1472.
(31) Fukuzumi, S.; Mori, H.; Imahori, H.; Suenobu, T.; Araki, Y.; Ito, O.; Kadish, K. M. *J. Am. Chem. Soc.* **2001**, *123*, 12458 and references therein.
(32) Zeng, Y.; Biczók, L.; Linschitz, H. *J. Phys. Chem.* **1992**, *96*, 5237.
(33) Arbogast, J. W.; Foote, C. S.; Kao, M. *J. Am. Chem. Soc.* **1992**, *114*, 2273.
(34) Suzuki, T.; Maruyama, Y.; Akasaka, T.; Ando, W.; Kobayashi, K.; Nagase, S. *J. Am. Chem. Soc.* **1994**, *116*, 1359.
(35) Guldi, D. M.; Hungerbühler, H.; Carmichael, I.; Asmus, K. D.; Magini, M. *J. Phys. Chem. A* **2000**, *104*, 8601.
(36) Hamann, T. W.; Bussandri, A.; van Willigen, H. Unpublished results.